Compensation of corneal aberrations by the internal optics in the human eye

Pablo Artal

Laboratorio de Optica, Universidad de Murcia,
Campus de Espinardo (Edificio C), 30071 Murcia, Spain

Antonio Guirao

Laboratorio de Optica, Universidad de Murcia,
Campus de Espinardo (Edificio C), 30071 Murcia, Spain

Esther Berrio

Laboratorio de Optica, Universidad de Murcia,
Campus de Espinardo (Edificio C), 30071 Murcia, Spain

David R. Williams

Center for Visual Science, University of Rochester,
Rochester, NY, USA 14627

The objective was to study the relative contribution of the optical aberrations of the cornea and the internal ocular optics (with the crystalline lens as the main component) to overall aberrations in the human eye. Three sets of wave-front aberration data were independently measured in the eyes of young subjects: for the anterior surface of the cornea, the complete eye, and internal ocular optics. The amount of aberration of both the cornea and internal optics was found to be larger than for the complete eye, indicating that the first surface of the cornea and internal optics partially compensate for each other's aberrations and produce an improved retinal image. This result has a number of practical implications. For example, it shows the limitation of corneal topography as a guide for new refractive procedures and provides a strong endorsement of the value of ocular wave-front sensing for those applications.

Introduction

Optical aberrations in the human eye impose a major physical limit on spatial vision. Interest in the study of ocular optics was evident centuries ago. Now the field is booming because of new optical technology to correct ocular aberrations beyond defocus and astigmatism. New technology could allow a generation of high-resolution ophthalmoscopes and better than normal vision with contact lenses or refractive surgery procedures customized to correct an individual's optical aberrations. Although a great deal of applied research is ongoing (Liang, Williams, & Miller, 1997; Vargas-Martín, Prieto, & Artal, 1998), fundamental questions concerning ocular aberrations remain unanswered. The answers to these questions will impact the development of these new ophthalmic technologies. For example, what are the relative contributions of aberrations in the crystalline lens and the cornea to the quality of images on the retina? Thomas Young, as early as 1801, performed an experiment in his own eye to measure the contribution of the lens to the ocular astigmatism (Young, 1801). He neutralized the corneal contribution by immersing his eye in water and found that his astigmatism persisted. In clinical practice, it is commonly accepted that the lens compensates for moderate corneal astigmatism. Recent studies, designed to separate aberrations of the cornea and the lens, concentrated on spherical aberration (El Hage & Berny, 1973; Tomlinson, Hemenger, & Garriott, 1993), or used only indirect estimates of the aberrations of the internal surfaces (Artal & Guirao, 1998), or were based on studies of crystalline lenses in vitro (Glasser & Campbell, 1998).

We performed three different and complementary sets of wave-front aberration (WA) measurements in the eyes of a group of healthy young subjects and showed clearly the relative contribution of the corneal surface and the internal optics of the eye to the ocular aberrations.

The WA is a function that characterizes the image-forming properties of any optical system (Born & Wolf, 1985). It is defined as the optical deviation of the wave front along a certain ray from the perfect spherical wave front. The WA is related to the image of a point source produced by the system (point-spread function [PSF]) through an integral equation (Goodman, 1996). First, the WAs of both the cornea and the complete eye were measured. By

combining these two sets of data, the aberrations of the internal optics were estimated by direct subtraction. Then the WA of the eye was measured after neutralizing the cornea using swimming goggles filled with saline water. The aberrations measured with the filled goggles correspond approximately to those of the internal ocular optics. The crystalline lens is the most important contributor to the aberrations of the internal ocular optics that also includes the posterior surface of the cornea and the ocular media.

Methods

Figure 1 shows a schematic diagram of the experimental procedure. From the aberrations of the complete eye and the cornea, those of the internal optics are estimated by direct subtraction. The aberrations of the internal optics are directly measured after neutralizing the aberrations of the first corneal surface.
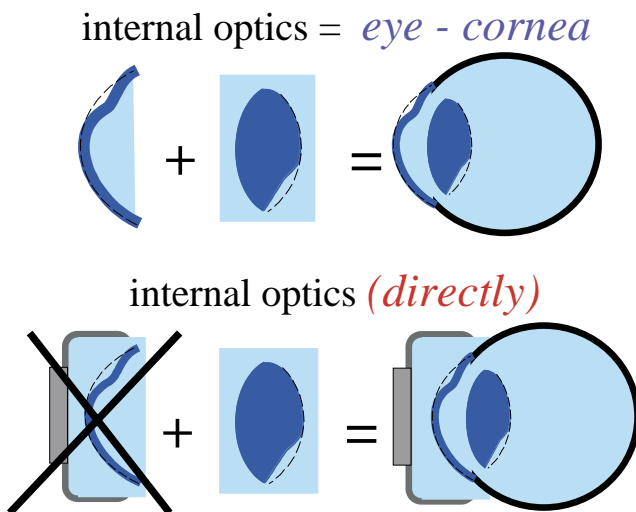

Figure 1. Schematic diagram of the experiments performed.

The WA of the eye was measured with a Hartmann-Shack (H-S) sensor (Liang, Grimm, Goelz, & Bille, 1994; Liang & Williams, 1997; Prieto, Vargas-Martín, Goelz, & Artal, 2000). A narrow infrared beam that acts as a beacon source is produced by a super-luminescent diode and is projected into the subject's retina. In the second pass, a microlens array, conjugated with the eye pupil, produces an image of spots on a charged-coupled device camera (CCD) (Figure 2A). The relative displacements of the spots are proportional to the WA local slopes. Then the WA is reconstructed as a Zernike polynomial expansion (Noll, 1976). The aberrations introduced by the anterior surface of the cornea were calculated from the corneal shape, measured by a videokeratographic device (MasterVue corneal topography system; Humphrey Instruments, San Leandro, CA). Once the anterior corneal surface was modeled, the difference in optical path between the chief ray and a marginal ray over the pupil yields the WA for the cornea (Guirao & Artal, 2000). From these two WA maps, the relative contributions of the cornea and the internal

optics to the overall ocular aberration were evaluated. The geometric center of the pupil was used as the reference point for the registration between H-S and corneal measurements. In a simple model with the two series of Zernike coefficients for the cornea and the eye, the aberrations of the internal optics were obtained by direct subtraction of each pair of coefficients. It was assumed that the wave aberrations were the same axially along small distances.

In addition, the WA for the internal optics was directly measured with the H-S sensor when refraction and aberrations of the corneal surface were cancelled by immersing the eye in saline water using swimming goggles (Millodot & Sivak, 1979). Light reached the eye through a hole along the optical axis of the goggles that was covered by a high-quality optical window. When the corneal surface power is cancelled, the eye becomes highly hyperopic. To obtain H-S images adequate for processing, this large defocus was compensated with a Badal optometer formed by two photographic objectives (Figure 2B). By using this procedure, several problems may affect the estimates of the aberrations of the internal optics. When the H-S sensor is used at the extreme vergence required for correcting the eye's hyperopia, the apparatus itself introduces large aberrations that may affect the results. This issue was overcome by using a reference image of the system, recorded in the same conditions, to compute the aberrations of the internal ocular optics. This removes any systematic aberrations present in the apparatus. In addition, the optical window placed in front of the goggles and the water act as a plane parallel plate that introduces spherical aberration for those vergences. The spherical aberration was calculated with a ray-tracing program and incorporated into the data analysis.
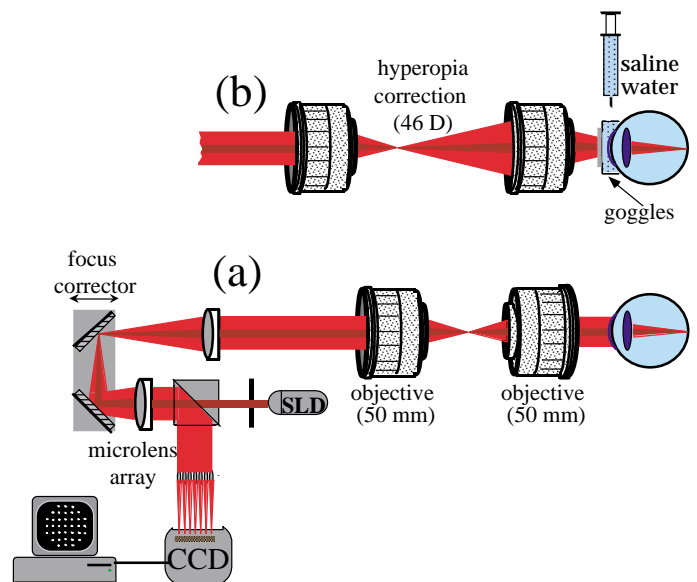

Figure 2. A. Schematic diagram of the Hartmann-Shack wave-front sensor used to measure the aberrations of the complete eye. SLD indicates super-luminescent source; CCD, charged-coupled device camera. B. Diagram of the part of the set-up modified to measure the aberration of the internal optics. The eye was equipped with swimming goggles filled with saline water. Defocus was compensated by the relative position of the two 50-mm objectives.

Figure 3 shows 2 examples of H-S images recorded in the naked eye (A) and in the eye with filled goggles (B). From independent measurements, we have the estimates of wave-front aberrations for the different optical components (anterior surface of the cornea and internal optics); therefore, the comparison of these estimates indicates the validity of the methods.
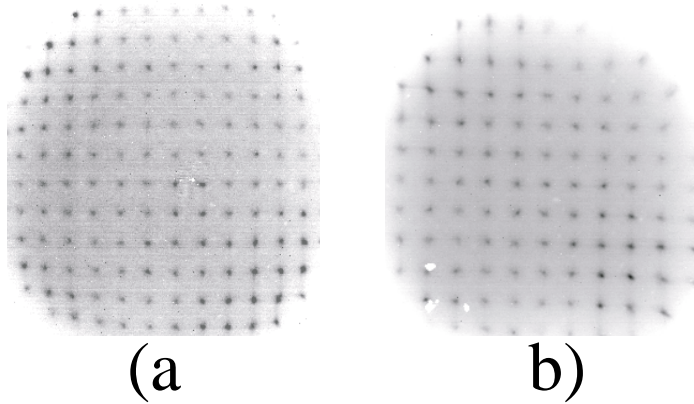

Figure 3. Examples of Hartmann-Shack image in the naked eye (A) and in the eye with filled goggles (B).

Aberrations of the cornea, measured both directly from the shape and by subtraction of the aberrations obtained with goggles from those of the whole, were found to be similar within the experimental variability. Figure 4 further explains this comparison. Figure 5 shows the Zernike coefficients of the aberrations for the anterior corneal surface obtained both directly (videokeratography) and indirectly (goggles) for 2 subjects. This result provides strong evidence for consistency of the complete procedure, supporting the simple model where corneal and internal optics aberrations are added in a single plane to produce the overall ocular aberrations.
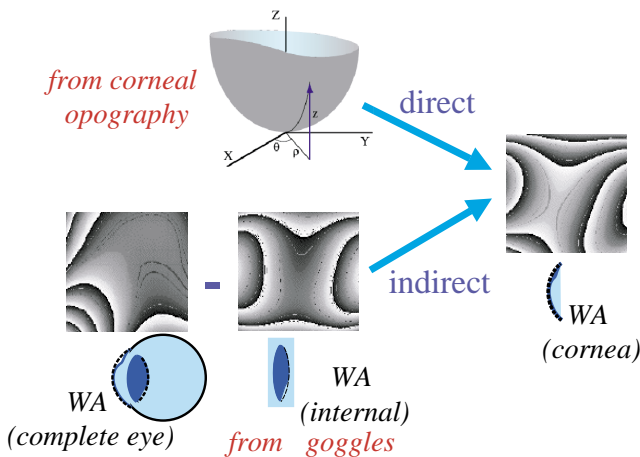

Figure 4. Schematic procedure to estimate the aberrations of the cornea directly and from indirect measurements (complete eye and anterior corneal surface).

We carried out the indirect set of measurements (with and without filled goggles) on the eyes of 5 subjects and the measurement of corneal and complete eye aberrations in another group of 6 subjects. In 2 of the subjects for which goggle measurements were performed, corneal topography for comparison (Figure 5) was also available. All of the subjects analyzed had normal vision (corrected visual acuity 1 [20/20] or better). Their ages ranged from 24 to 38 years. The study followed the tenets of the Declaration of Helsinki, and signed informed consent was obtained from every subject after the nature and all possible consequences of the study had been explained. The H-S images were recorded with paralyzed accommodation (using cyclopentholate 1%) and infrared light (780 nm). The aberrations were estimated for different pupil diameters (4.7 mm when aberrations of the internal optics were obtained directly from the goggle experiment and 5.9 in the remainder of the cases).
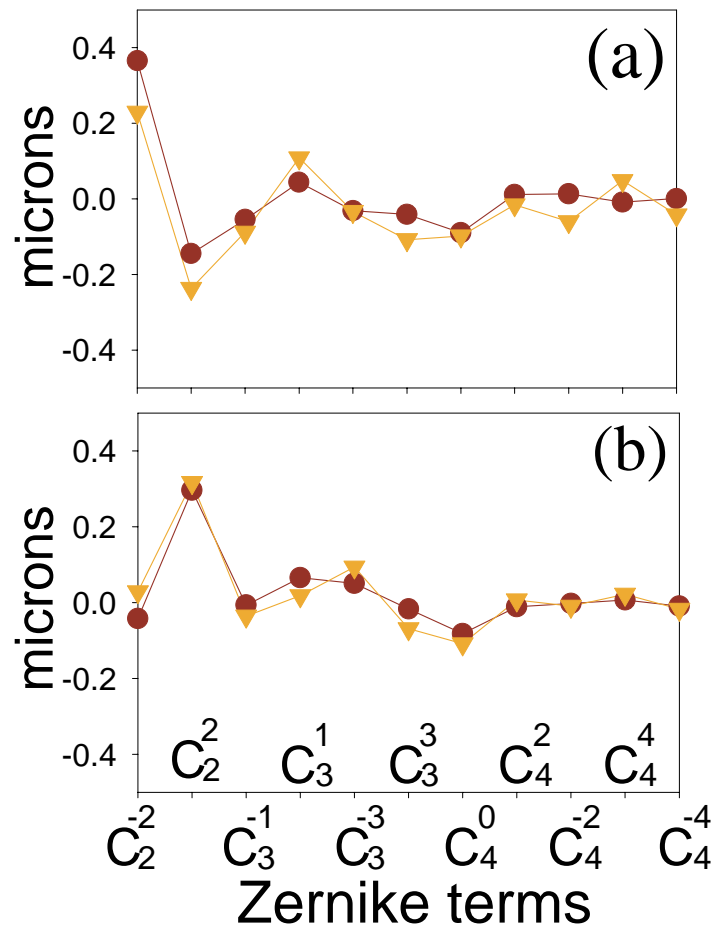

Figure 5. Zernike coefficients of the aberrations of the cornea for 2 subjects, obtained from the shape (circles) and by subtraction of the aberrations of the whole eye and the internal surfaces (triangles), as described in Figure 4.

Results

The results presented in this section are direct measurements of the aberrations of the anterior corneal surface and the complete eye, and indirect estimates of the aberrations of the internal surfaces. Figure 6 shows a representative example of the results for 1 of the subjects: the WA maps for the cornea (A), the internal optics (B), and the complete eye (C) together with their associated PSFs calculated at the best image plane (D-F). In this subject, the magnitude of aberrations is larger in the cornea than in the complete eye. This can be easily noted in the wrapped representation of the WAs by counting the number of phase-steps appearing in the maps for the cornea and for the complete eye, or, alternatively, by comparing the spreads of the associated PSFs.

Figure 7 shows the Zernike terms for the aberrations of the cornea (solid symbols) and the internal optics for all subjects. The magnitude of the most important aberration terms is similar for the two components, but with a change in sign. This produces an eye with smaller amounts of aberrations than its main components, indicating that the internal optics partially compensate for the aberrations of the anterior surface of the cornea. Figure 8 shows the root mean square of the WA (a parameter indicating the magnitude of the aberration) for the eye, the anterior surface of the cornea, and the internal optics for 6 eyes after defocus was removed. In every case, the aberrations of the corneal surface and the isolated internal optics are larger than those of the total eye.
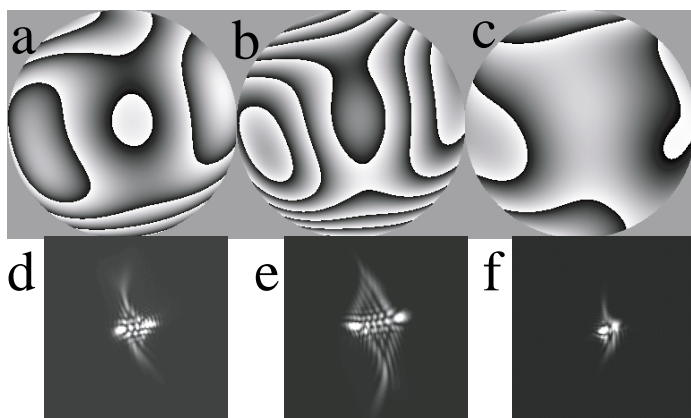

Figure 6. A-C. Wave-front aberration (WA) maps for the cornea (A), the internal optics (B) and the complete eye (C). These WAs are represented as modulo-π. The pupil diameter was 5.9 mm. D-E. Associated point-spread functions (PSFs) calculated at the best image plane from WA panels A-C. Each image subtends 20 minutes of arc of visual field.
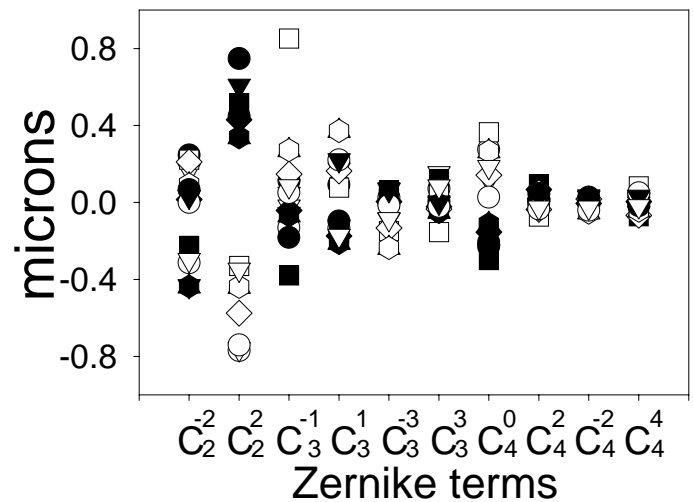

Figure 7. Zernike terms for the cornea (solid symbols) and the internal optics (open symbols) for all subjects.
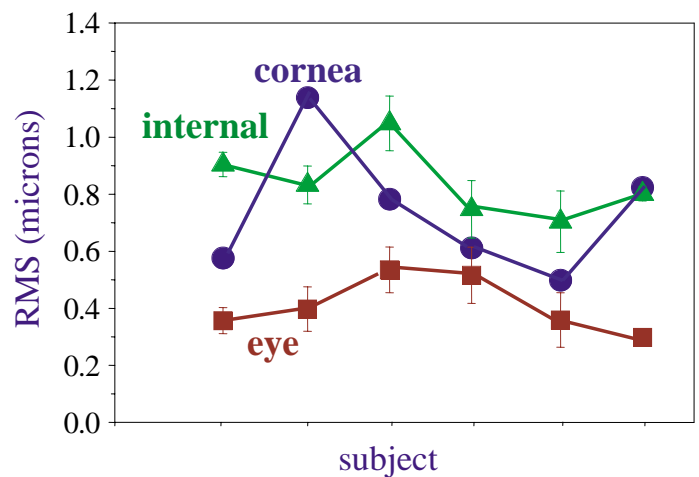

Figure 8. Root mean square of the wave-front aberration of the eye (squares), the cornea (circles), and the internal optics (triangles) for 6 eyes after defocus was removed.

Figure 9 shows the values of the Zernike terms up to fourth order (from 5 to 14) for all subjects for the corneal surface versus the internal optics. There is a significant negative correlation between corneal and internal optics aberrations (regression coefficient, 0.86). This result indicates a significant coupling of individual aberration terms between the cornea and the internal ocular optics. Astigmatism for the cornea and internal optics (Zernike terms 5 and 6) had opposite signs. Figure 10 shows the astigmatism of the corneal surface versus the internal optics. This supports a well-known fact in clinical practice: the internal optics tend to compensate for the corneal astigmatism. However, what is more surprising is that this compensation also takes place for higher order aberrations. Third- and fourth-order aberrations were also partially compensated. A large fraction of the spherical aberration of the cornea is cancelled by the internal optics. The magnitude of comalike aberrations of the cornea is also significantly reduced by the internal optics. Figure 11 shows

the values of third-order coma and triangular astigmatism for the cornea versus the internal surfaces. Figure 12 shows the fraction of the spherical aberration and coma in the cornea that is compensated by the internal surfaces.
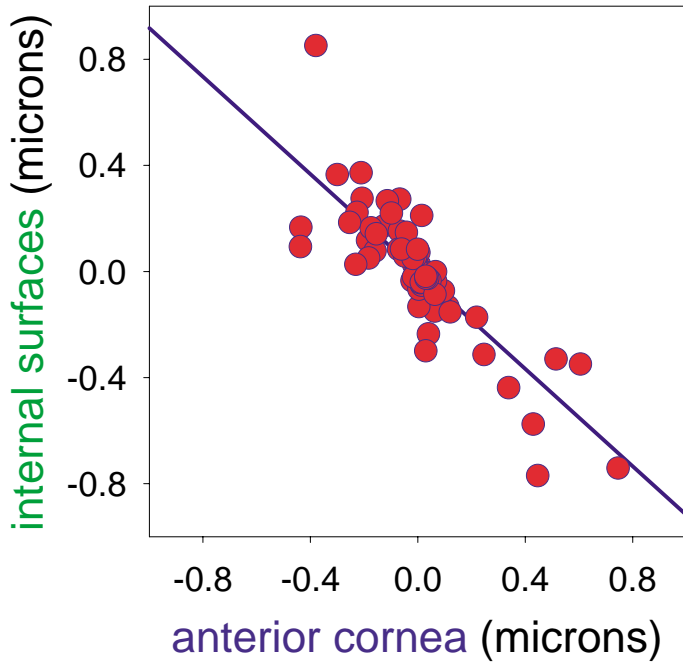

Figure 9. Values of Zernike terms up to fourth order (5-14) for the aberrations of the cornea versus the internal optics for all subjects.
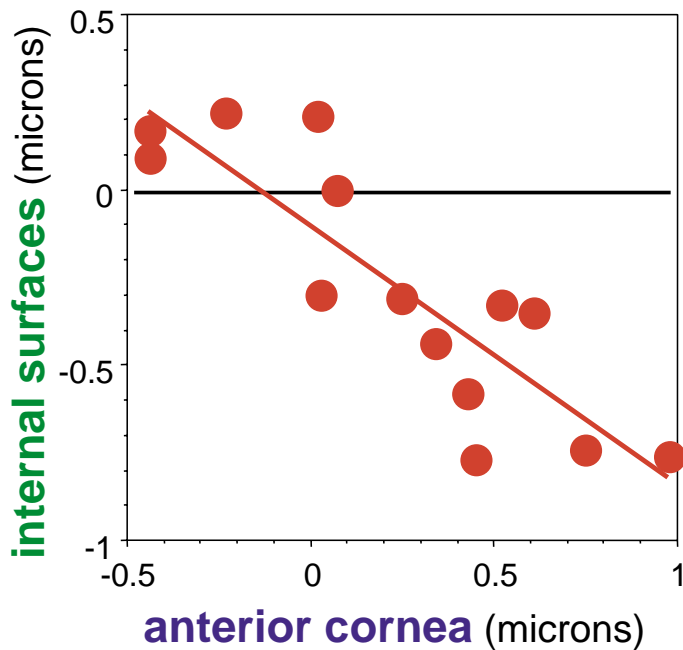

Figure 10. Values of astigmatism for the cornea versus the internal optics for all subjects.
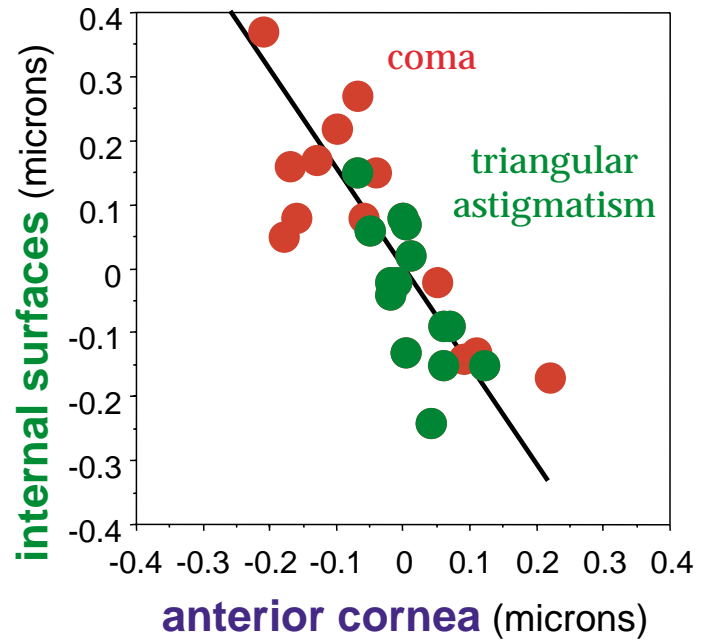

Figure 11. Value of third-order coma and triangular astigmatism for the cornea versus the internal optics for all subjects.
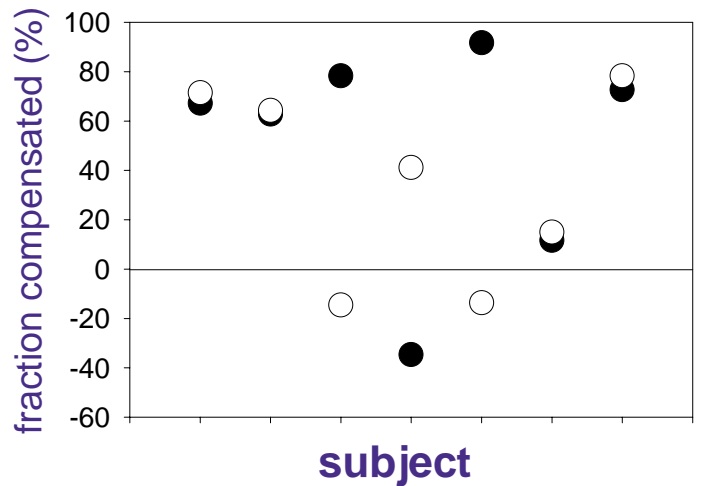

Figure 12. Fraction of spherical aberration (solid circles) and coma (open circles) of the cornea that are compensated by the internal surfaces in every subject.

Discussion

This balance of corneal and internal aberrations represents a typical example of a coupling of 2 optical systems. In this case, the corneal surface and the internal ocular optics, both with a relative poor optical quality, combine to form a system with a better optical performance. In optical engineering, a series of lenses in cascade are usually used to optimize the overall quality of the system (Smith, 1990); however, the situation in the eye is different in that there is not a simple access to every lens as

a separate component. How this optical quality optimization occurs in the human eye is not clear. One can imagine either an active process or that the compensation is simply a passive consequence of some random positioning of the ocular elements.

The distributions of astigmatism and spherical aberration reveal systematic patterns in the population of eyes (ie, opposite sign of the spherical aberrations of corneal and internal optics [Zernike terms 5, 6, and 11 in Figure 7]). This may suggest an evolutionary process to reach an optimum balance for those aberration terms. However, other aberrations, such as coma, seem to distribute randomly from subject to subject, favoring a passive compensation process or perhaps one in which active compensation can occur during development.

There are not enough precise data on the shape, location, and refractive index of every ocular component to determine the physical basis for the compensation. However, a simple model provides a general picture of what could be happening in a normal, nearly emmetropic young eye. The corneal surface has spherical aberration and a certain amount of astigmatism and comalike aberrations with orientation and magnitude varying from subject to subject. Internal optics can be understood as the lens, which when isolated presents only spherical aberration similar in magnitude to that of the cornea but with opposite sign. An optical element with only fourth-order spherical aberration generates lower-order terms (comalike, astigmatism, defocus, and tilts) when it is decentered (López-Gil, Howland, Howland, Charman, & Applegate, 1998) or tilted with respect to the axis. Small decentering and tilts of the lens produce aberrations with a similar magnitude for the internal optics that we measured. This simple model may explain how the compensation is achieved: the lens moves and tilts slightly to compensate in part for the aberrations of the cornea. Though the eye is sophisticated enough to maintain emmetropia by controlling eye growth during development, it is not clear that it is also sophisticated enough to improve retinal image quality through subtle control of lens position during development.

Other possible mechanisms could be involved in the compensation we found. One is the possible effect on the aberration of the posterior corneal surface. It should be noted that what we referred to as "internal ocular optics" also includes the posterior surface of the cornea (Guirao & Artal, 2000). The difference in refractive index between the cornea and the aqueous humor is about 10% of the difference of indexes between air and cornea. It is, therefore, unlikely that the posterior corneal surface makes a significant contribution to the aberrations. However, if

the posterior surface of the cornea has a shape similar to the first surface, because the refractive index change is opposite, a small amount of first-surface aberration could be compensated. Precise measurements of both corneal surfaces would allow determination of the posterior surface's exact role in the aberrations. A decentration of the eye's pupil could also explain part of the balance obtained between cornea and internal surfaces. If both corneal and ocular aberrations were measured with respect to the eye's pupil and this were decentered, we could expect a coma aberration produced by the spherical aberration of the cornea and also a coma with opposite sign produced by the spherical aberration of the internal surfaces. However, corneal aberrations were measured with respect to the corneal pole; in the subjects studied, the corneal pole and the center of the pupil were close enough that we did not anticipate an effect as large as we observed. Other types of misalignments between the optical elements of the eye could work similarly, and might explain the compensation.

To investigate whether a random distribution of aberrations in the crystalline lens could by chance compensate for the corneal aberrations, we simulated 1000 lenses with random coma (magnitude and orientation normally distributed). We mathematically coupled the corneal aberrations of each subject with those of the randomly aberrated lens. The normally distributed coma value in the lens that produces a larger compensation is the one with standard deviation equal to the average corneal coma. Even for this case, we did not find any instance of a reduction in the total aberration of the eye. These calculations showed that the compensation between cornea and lens could not be attributed to purely random processes.

Although the number of subjects in this study is relatively small, the negative correlation found in Figure 9 represents a statistical argument in favor of the compensation for each of these aberrations. The balance of aberrations between the cornea and the internal optics that we found in this study may explain some facts that are not well understood. One example is the optical performance of eyes after implantation of intraocular lenses. These lenses have extremely good image quality when measured in an optical bench, but the final optical performance in the implanted eye is lower than expected (Artal, Marcos, Navarro, Miranda, & Ferro, 1995). Clearly, the ideal substitute for the natural lens is not a lens with the best optical performance when isolated, but a lens designed to compensate for the aberrations of the cornea (Figure 12). This result has important implications for ophthalmic applications. To maximize the quality of the retinal image, intraocular and contact lenses should be designed with an

aberration profile matching that of the cornea or the lens. In addition, to achieve the optimum retinal image, procedures in refractive surgery should ablate the cornea based on the overall ocular aberrations rather than the corneal aberrations.
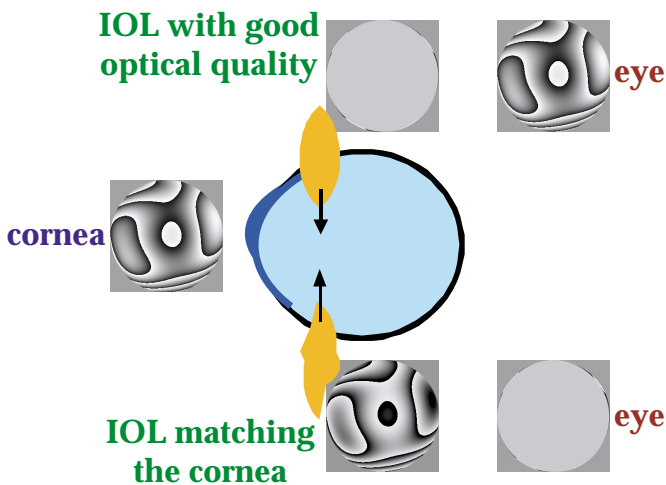

Figure 13. Schematic illustration of the effect of the coupling of corneal and intraocular lenses (IOL) aberrations.

Remarkably, the aberration compensation found in young subjects' eyes is not generally present in older eyes (Berrio, Guirao, Redondo, Piers, & Artal, 2000). The amount of aberrations of the whole eye increases with age (Artal, Ferro, Miranda, & Navarro, 1993; Guirao et al, 1999); however, while the aberrations are larger for the cornea than for the eye in young cases, as we have shown, this is usually not the case for older subjects. This indicates that as the eye gets older, the aberrations of ocular components decouple, which may be responsible for the overall deterioration of ocular optics over the life span.

Additional questions have arisen concerning the nature of this aberration balance. Is it produced during the earlier stages of the development of the eye, remaining stable during adulthood until normal aging breaks the balance? Or, alternatively, is there a certain plasticity to compensate aberrations in the young adult eye if any changes in the aberrations of any ocular component occur? Whether or not this compensation is an active or passive process also remains to be clarified.

Acknowledgments

References

Artal, P., Ferro, M., Miranda, I., & Navarro, R. (1993). Effects of aging in retinal image quality. *Journal of the Optical Society of America A, 10*, 1656-1662.

Artal, P., & Guirao, A. (1998). Contributions of the cornea and lens to the aberrations of the human eye. *Optics Letters, 23*, 1713-1715.

Artal, P., Marcos, S., Navarro, R., Miranda, I., & Ferro, M. (1995). Through focus image quality of eyes implanted with monofocal and multifocal intraocular lenses. *Optics Engineering, 34*, 772-779.

Berrio, E., Guirao, A., Redondo, M., Piers, P., & Artal, P. (2000). The contribution of the corneal and internal optics aberrations changes with age. *Investigative Ophthalmology and Visual Science*, Suppl. 41, S545.

Born, M., & Wolf, E. (1985). *Principles of Optics*. New York: Pergamon.

El Hage, S. G., & Berny, F. (1973). Contribution of the crystalline lens to the spherical aberration of the eye. *Journal of the Optical Society of America, 63*, 205-211.

Glasser, A., & Campbell, M. C. W. (1998). Presbyopia and the optical changes in the human crystalline lens with age. *Vision Research, 38*, 209-229.

Goodman, J. W. (1996). *Introduction to Fourier Optics*, (2nd ed.). New York: McGraw Hill.

Guirao, A., & Artal, P. (2000). Corneal wave aberrations from videokeratography: accuracy and limitations of the procedure. *Journal of the Optical Society of America A, 17*, 955-965.

Guirao, A., Gonzalez, C., Redondo, M., Geraghty, E., Norrby, S., & Artal, P. (1999). Average optical performance of the human eye as a function of age in a normal population. *Investigative Ophthalmology and Visual Science, 40*, 197-202.

Liang, J., Grimm, B., Goelz, S., & Bille, J. F. (1994). Objective measurement of the WA's aberration of the human eye with the use of a Hartmann-Shack sensor. *Journal of the Optical Society of America A, 11,* 1949-1957.

Liang, J., & Williams, D. R. (1997). Aberrations and retinal image quality of the normal human eye. *Journal of the Optical Society of America A, 14,* 2873-2883.

Liang, J., Williams, D. R., & Miller, D. T. (1997). Supernormal vision and high-resolution retinal imaging through adaptive optics. *Journal of the Optical Society of America A, 14,* 2884-2892.

López-Gil, N., Howland, H. C., Howland, B., Charman, N., & Applegate, R. (1998). Generation of third-order spherical aberration and coma using radially symmetric fourth-order lenses. *Journal of the Optical Society of America A, 15,* 2563-2571.

Millodot, M., & Sivak, J. (1979). Contribution of the cornea and the lens to the spherical aberration of the eye. *Vision Research, 19,* 685-687.

Noll, R.J. (1976). Zernike polynomials and atmospheric turbulence. *Journal of the Optical Society of America, 66,* 207-211.

Prieto, P.M., Vargas-Martín, F., Goelz, S., & Artal, P. (2000). Analysis of the performance of the Hartmann-Shack sensor in the human eye. *Journal of the Optical Society of America A, 17,* 1388-1398.

Smith, W.J. (1990). *Modern Optical Engineering* (2nd ed.). New York: McGraw Hill.

Tomlinson, A., Hemenger, R. P., & Garriott, R. (1993). Method for estimating the spheric aberration of the human crystalline lens in vivo. *Investigative Opthalmology and Visual Science, 34,* 621-629.

Vargas-Martin, F., Prieto, P., & Artal, P. (1998). Correction of the aberrations in the human eye with liquid crystal spatial light modulators: limits to the performance. *Journal of the Optical Society of America A, 15,* 2552-2562.

Young, T. (1801). On the mechanism of the eye. *Philosophical Transactions of the Royal Society of London, 91,* 23-88.